

Title	Fatigue Strength of Field-welded Joints of U-shaped Trough Rib for Bridge Deck(Welding Mechanics, Strength & Design)
Author(s)	Horikawa, Kohsuke; Lee, Dong uk; Ishizaki, Hiroshi
Citation	Transactions of JWRI. 1983, 12(2), p. 287-294
Version Type	VoR
URL	https://doi.org/10.18910/7936
rights	
Note	

Osaka University Knowledge Archive : OUKA

<https://ir.library.osaka-u.ac.jp/>

Osaka University

Fatigue Strength of Field-welded Joints of U-shaped Trough Rib for Bridge Deck[†]

Kohsuke HORIKAWA*, Dong uk LEE** and Hiroshi ISHIZAKI***

Abstract

Thin-walled closed section is very useful for steel bridges deck to do warping rigidity and load distribution. However, there are a kind of thin-walled closed section that is U-shaped trough rib to be easy of misalignment for its field-welded joint.

This paper describes experiments relating to the fatigue lives of field welded U-shaped trough rib to deck plate joints in bridge deck, under transverse bending and tensile fatigue strength. The investigation involved fatigue test on full scale specimen and tensile fatigue specimen that were subjected to constant amplitude loading.

The main finding is investigation of crack initiation and propagation of trough rib with backing strip under the action of a partial moment by misalignment. The analysis of full scale model and tensile fatigue specimen model were used by Finite-element method. Both the experiment and the analysis of FEM, the stress concentrated weld root of inside corner of U-shaped trough rib.

KEY WORDS: (Misalignment) (Fatigue Life) (Life-to-crack-initiation) (Striation Pattern) (Beach Mark) (Root Angle) (Fish Eye) (Shear Lag) (Stress Influence Coefficient) (Stress Concentration Ratio)

1. Introduction

Closed U-shaped trough rib is useful for steel plate deck of warping rigidity, having many kind of floor system¹⁾. Welding that field connection of deck plate for pavement is the most desirable, and the fatigue strength of welded joints has been investigated extensively in the past. However, trough rib and deck plate are often welded at same time in field. Field welding of U-shaped trough ribs are connected by overhead welding, partial welded with backing strip. In this case, it easy to occur weld defects, misalignment and root gap. Above that reason, fatigue lives shorten²⁾, and crack initiation developed at root inside corner of U-shaped trough rib³⁾.

This paper deals with bending fatigue life in relation to misalignment of full-scale closed U-shape trough rib, also the relationship between tensile fatigue life and welding procedure was studied. In order to investigate stress concentration, the elastic analysis of full scale specimen and tensile fatigue specimen employed the finite element method. The finite-element model for these specimens were composed of two-dimensional or three-dimensional, constant stress, triangular elements.

2. Fatigue Strength of Full-scale Specimens

2.1 Identification and material

The specimen were made from mild steel, equivalent to JIS SS3104 and ASTM A36. The shape of specimen shown in Fig. 1 and its identification was summarized in Table 1.

All of the trough rib are cold-formed from a flat plate by press, and the radius(R) of corner is 30 mm. Low hydrogen type electrode of 3.2 and 4.0 mm dia. (LB 26 equivalent to AWS E7016) was used for welding trough

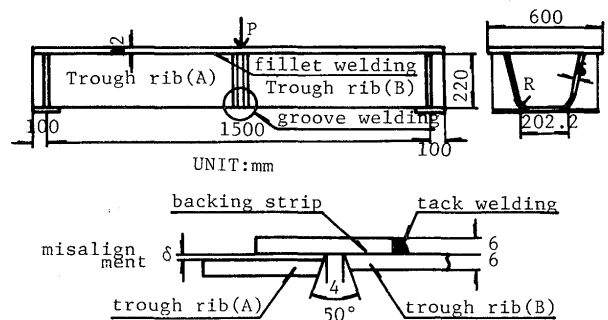


Fig. 1 Bending fatigue specimen of closed U-shaped trough rib.

Transactions of JWRI is published by Welding Research Institute of Osaka University, Ibaraki, Osaka 567, Japan

[†] Received on October 31, 1983

* Associate Professor

** Graduate Student of Osaka University

*** Han Shin Expressway Public Corporation

Table 1 Summary of bending fatigue test

Specimen number.	Cycle (X10 ⁻⁴)		Root gap (mm)	Misalignment	*JIS Grade	Stress of bottom flange		Endurance cycle (10 ⁴)		Remark
	P=2-18t	P=10-18				σ_{max}	$\Delta\sigma_{range}$	N _i	N _f	
A-1	50	10	4.0	0	1st	16.58	14.74	400-450	587	P=2-26t 3X10 ⁶ discon. 28X10 ⁵ "
A-2			"	0.5	2nd				83	
A-3	50	10	"	0	1st	23.95	22.11			
A-4	20	10	"	0	1st	"	"			
B-1	20	5	"	2.0	1st	"	"	60-80	140	
B-2	20	5	"	4.0	1st	"	"	20below	38	
C	20	0	"	0.6	1st	"	"	260-280	322	
D	20	0	"	1.0	2nd	"	"	80-100	169	
E	20	10	"	1.5	4rd	"	"	100-120	146	
F-1	20	0	"	0.4	2nd	"	"	240-260	349	
F-2	10	10	"	0	2nd	"	"			32X10 ⁵ discon.
G	20	0	"	1.0	2nd	"	"	160-180	264	P=2-26t
H-1	20	20	"	0.8	2nd	"	"	100-120	190	
H-2			"	0.2	2nd	"	"		163	

*JIS Z3104(Method of radiographic test and classification of radiographs for steel welds)

rib A and B with manual metal welding of overhead position. Deck plate and trough rib were welded the same electrodes and same welding procedure as trough A and B. The welding procedure simulates the field welding.

2.2 Experimental procedure

Load range $P=16^t$ (2-18^t) and $P=24^t$ (2-26^t) correspond to the nominal mean stress at the bottom flange of the trough rib.

(a) $P=16^t$

$$\sigma_{max} = 16.58 \text{ Kg/mm}^2$$

$$\sigma_{min} = 1.84 \text{ Kg/mm}^2$$

$$\Delta\sigma_{range} = 14.74 \text{ Kg/mm}^2$$

(b) $P=24^t$

$$\sigma_{max} = 23.95 \text{ Kg/mm}^2$$

$$\sigma_{min} = 1.84 \text{ Kg/mm}^2$$

$$\Delta\sigma_{range} = 22.11 \text{ Kg/mm}^2$$

All of the test was performed under constant amplitude loading with Servohydraulic testing machine. (Capacity 20 ton: Saginomiya Seisakusho, Inc.)

2.3 Loading-Strain measurement

Figure 2a shows strain gauge position at the bottom flange of the trough rib. Bottom strain were measured every 100 thousands or 500 thousands cycles for each specimens, respectively (Table 1). Therefore, it can be predicted of fatigue life-to-crack initiation, if the difference of strain is large whenever unloading or loading after fatigue test with 100 thousands or 500 thousands cycle.

For example, Fig. 2b shows that difference of strain occurred large between ⑫ and ⑬ at strain gauge S₄. As also there is great difference between ⑫ and ⑬ at strain gauge S₄ as shown in Fig. 2c. Both Fig. 2b and Fig. 2c

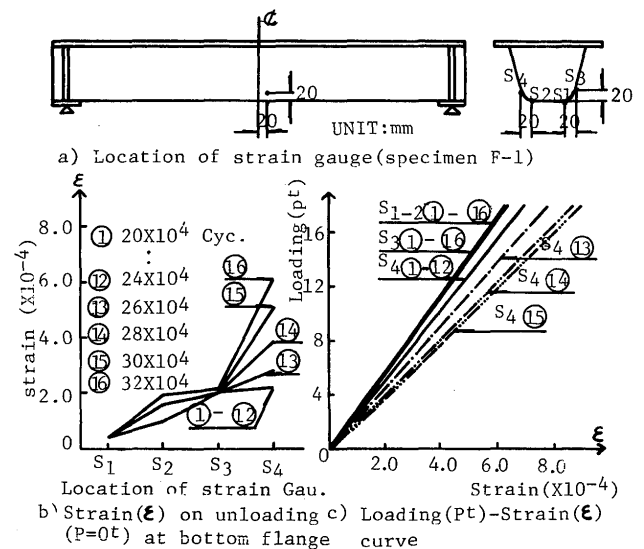


Fig. 2 Strain on bottom flange for each unloading step (Specimen F-1)

notes that difference of strain occurred large between ⑫ and ⑬ at strain gauge S₄.

2.4 Results of bending fatigue test

The results of bending fatigue test are summarized in Table 1. Relationship between the stress range and fatigue lives were shown in Fig. 3, and Fig. 4 described its misalignment and fatigue lives. From Fig. 4 it is clear that the more misalignment is large the more fatigue lives will be shorten³⁾.

2.5 Observing crack initiation and propagation

Total of 14 specimens are tested, among that 11 specimens are failed as shown in Table 1. Fatigue crack of all failed specimen was initiated at welding root of inside of trough rib.

(1) Scanning electron microscope (specimen B-1)

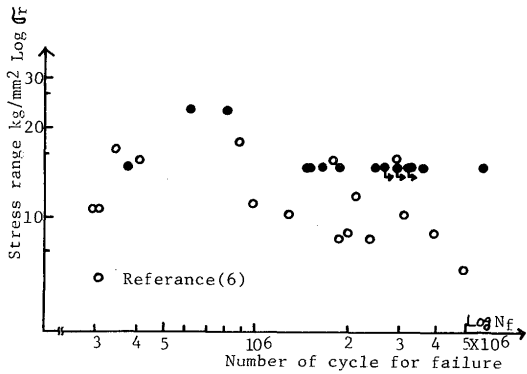


Fig. 3 Fatigue test results

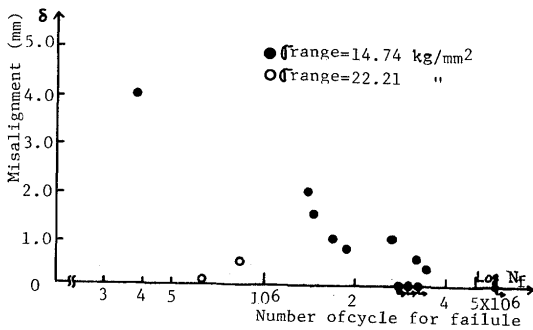


Fig. 4 Relationship between misalignment and fatigue life

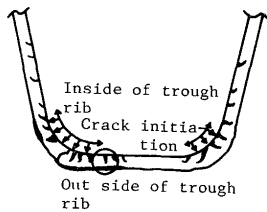


Fig. 5 Sketch of crack initiation and propagation (Specimen B-1)

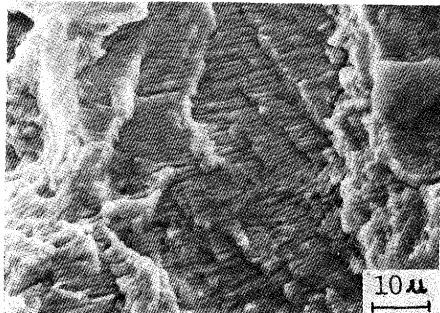


Fig. 6 Fatigue striations pattern crack growth direction is down

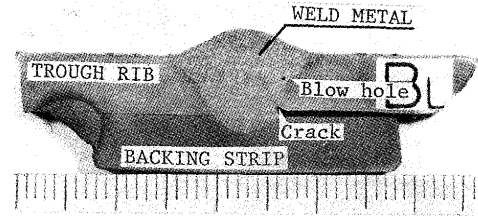


Fig. 7 Macro section of welding root corner

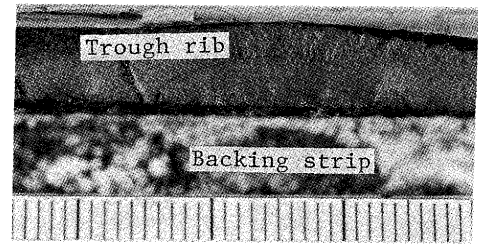


Fig. 8 Beach mark (crack developed at inside trough rib)

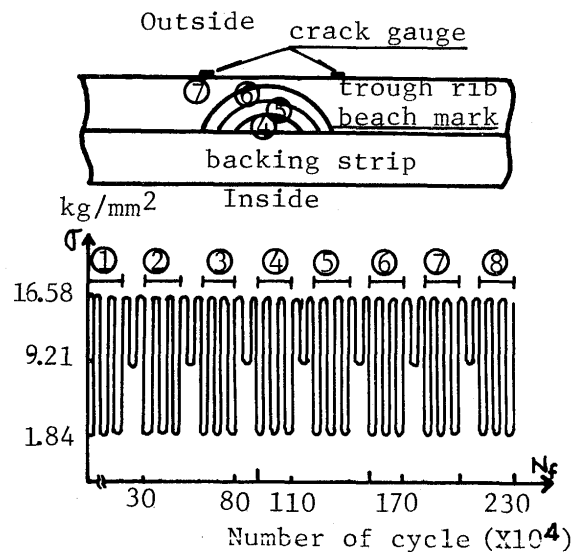


Fig. 9 Life-to-crack propagation by beach mark

At first, numerous cracks was initiated at the inside corner of trough rib as shown in Fig. 5, and they was propagated to the outside trough rib step by step. Finally, it shows that they was extended to both side of corner³⁾. Very high magnification micrographs of fatigue striations caused by constant amplitude load cycling are shown in Fig. 6⁴⁾⁵⁾. Such regular striation patterns provide evidence of the mechanism of progressive crack extension per load cycle and were reported by many authors for a variety of metals⁶⁾.

(2) Macro section (specimen C)

At first, the crack was developed at a corner and it was propagated into the opposite corner of base

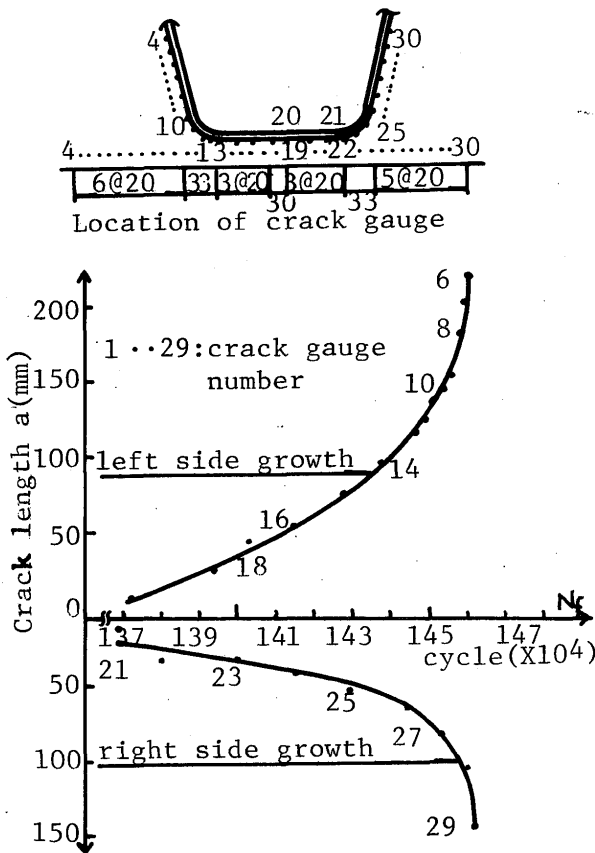


Fig. 10 a ~ N curve

metal. As shown in Fig. 7, it was found that the crack was initiated from weld root of inside corner of trough rib. Also, blow hole could be observed in weld metal, but it was not the cause of crack initiation.

(3) Beach mark (specimen E)

Beach mark was observed near the corner of bottom flange. Fig. 8 and Fig. 9 show life-to-crack-progation. According to beach mark, crack was initiated from inside corner, propagated outside.

(4) Crack length(a)-Fatigue life(N_f)

Crack propagation was investigated by crack gauge attached to outside of trough (Fig. 10). At first crack gauge was cut off No.21 and continued No. 21 → 19 . . , while a few minute late No.22 was cut off, and then propagated No.23 → 24 . . . (Fig. 10).

3. Fatigue Strength of tensile specimen

3.1 Test specimen of tensile fatigue

Fatigue specimen type is shown in Fig. 11 and specimens identification as shown in Table 2 were manufactured from JIS SS41 steel. In Table 2, H-series are Manual Metal Arc Welding, C-series are CO₂ Semi-automatic Arc Welding, M-series are Metal Active Gas Arc Welding

(Ar+20%CO₂). B-14 is 40 Kg/mm²-grade illuminate, LB-47A and LB-52 correspond to AWS 7016, DW-100 to E 70T-1, MIX-50 to E 70S-3, and RP is reverse polarity.

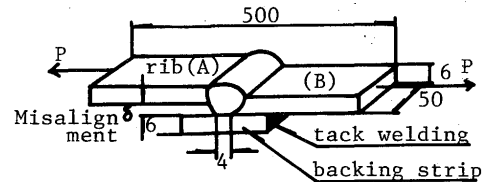


Fig. 11 Fatigue specimen (All measurements in millimeters)

Table 2 Specimen identification

mm	0	2	3	4	Total
H:B-14		2			2
H:LB-47A	2	4	2	2	10
H:LB-52		2			2
C:DW-100RP	2	4	2	2	10
C:DW-100SP		2			2
M:MIX-50S		2			2
Total	4	16	4	4	28

3.2 Results of tensile fatigue test

Fatigue test results of all 28 tensile specimens are described in Fig. 12. Tensile strength correspond to bottom flange of section 2.2 ($\sigma_{max}=16.58 \text{ Kg/mm}^2$, $\sigma_{min}=1.84 \text{ Kg/mm}^2$, $\Delta\sigma \text{ range}=14.74 \text{ Kg/mm}^2$, $k=0.111$). All testing was carried out under constant amplitude loading with Servohydraulic testing machine (Shimazu servo pulser EHF-E20).

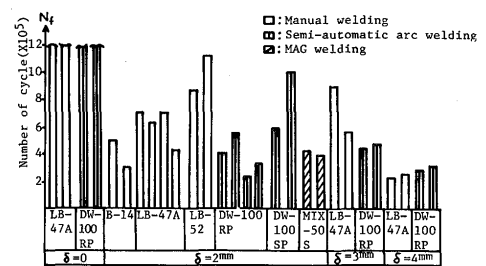


Fig. 12 Fatigue test results

1.84 Kg/mm², $\Delta\sigma \text{ range}=14.74 \text{ Kg/mm}^2$, $k=0.111$). All testing was carried out under constant amplitude loading with Servohydraulic testing machine (Shimazu servo pulser EHF-E20).

- (1) Relationship between misalignment and fatigue life
 - a) In case of LB-47 A: misalignment 2 mm \doteq misalignment 3 mm > misalignment 4 mm.
 - b) In case of DW-100 (RP): misalignment 2 mm \doteq misalignment 3 mm > misalignment 4 mm.
- (2) Relationship between welding process, welding electrode and fatigue life

- a) In case of $\delta=2$ mm and manual welding: LB-52 is the highest fatigue strength.
- b) In case of $\delta=2$ mm and Semi-automatic Arc Welding: Fatigue strength of SAAW DW-100 (SP) is higher than SAAW DW-100 (RP).
- c) $\delta=3$ mm: Fatigue strength of manual welding (LB-47A) is higher than SAAW DW-100 (RP).
- d) $\delta=4$ mm: Fatigue strength of SAAW DW-100 (RP) is slight higher than manual welding (LB-47 A).

3.3 Crack initiation

Among 24 failed specimens, fatigue crack of 20 specimens was developed from weld root with backing strip and 4 specimens was initiated at weld toe of trough rib.

- (1) The fatigue crack was initiated mainly at the weld root of specimen as shown in Fig. 13⁷⁾.
- (2) A slight fish eye was observed at MAG welding (MIX-50S) as shown in Fig. 13, but it did not cause the crack initiation, and then blow hole and slag inclusion were observed in other specimens. However, they did not cause crack development⁷⁾.
- (3) In spite of same welding condition, there were various root types according to macro section (θ_1) and micro section (θ_2) as shown in Table 3. Accordingly, by changing both misalignment (δ) and root angle (θ_1), they were analyzed plane isotropic elastic using Finite Element Method.

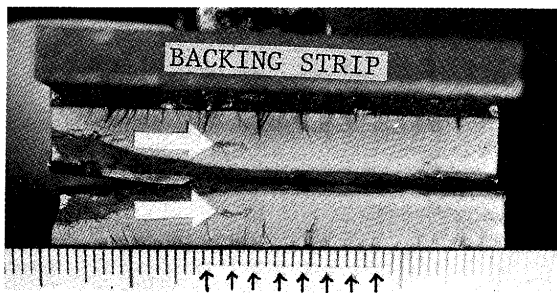


Fig. 13 Fatigue fracture surface (Arrow is fish eye)

Table 3 Macro angle (θ_1), Micro angle (θ_2) and root radius (ρ)

Welding rod	Misalignment	Macro angle (θ_1)	Micro ang. (θ_2)	ρ mm	Remark		
B-14	2	135.0	158.3	0.107			
LB-47A	2	116.6	151.6	0.188			
	2	73.3	142.8	0.286			
	3	88.7	140.2	0.391			
	4	71.8	123.5	0.084			
LB-52	2	90.0	131.2	0.086			
	DW-100	2	44.0	150.7		0.078	
		RP	2	65.1		158.1	0.676
		3	58.2	137.2		0.583	
4	68.2	150.0	0.275				
SP	2	87.0	147.6	0.567			
MIX-50S	2	55.2	143.5	0.229			

4. Finite-element Analysis of Stress Concentration Zone

4.1 FEM Analysis of full scale model

Three different types on full scale model of section 2 were analyzed using 3-dimensional FEM as shown in Fig. 14;

I) Non-misalignment with non-backing strip, II) Non-misalignment with backing strip, III) Misalignment ($\delta=2$ mm) with backing strip.

Figure 15 shows Stress Influence Coefficients (ξ : X-direction) on connecting zone when loading is 10000 kg and misalignment ($\delta=2$ mm), and then, Fig. 16 indicates the best stress influence coefficients (ξ) for I) II) III).

The distribution of tensile stress across the width of all cases did not be uniform, but, as in Fig. 15, higher at the corner than the bottom flange. It is well-known as SHEAR LAG^{1) 8)}, since it involves a shear deformation in the trough rib.

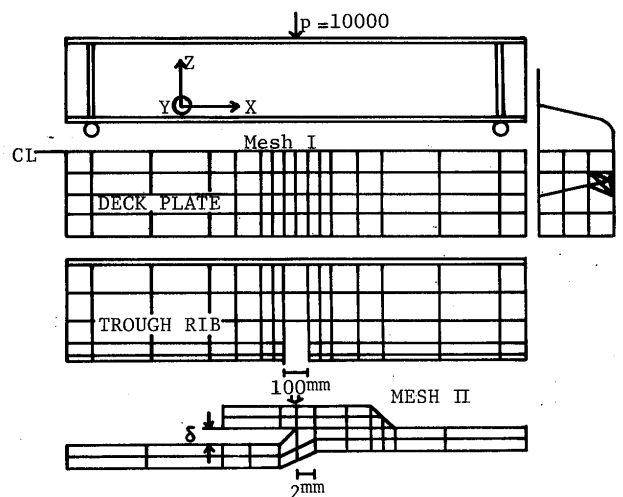


Fig. 14 FEM Model

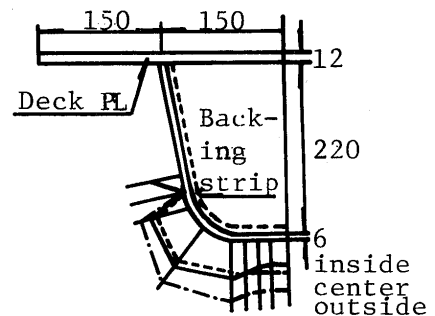


Fig. 15 Shear lag

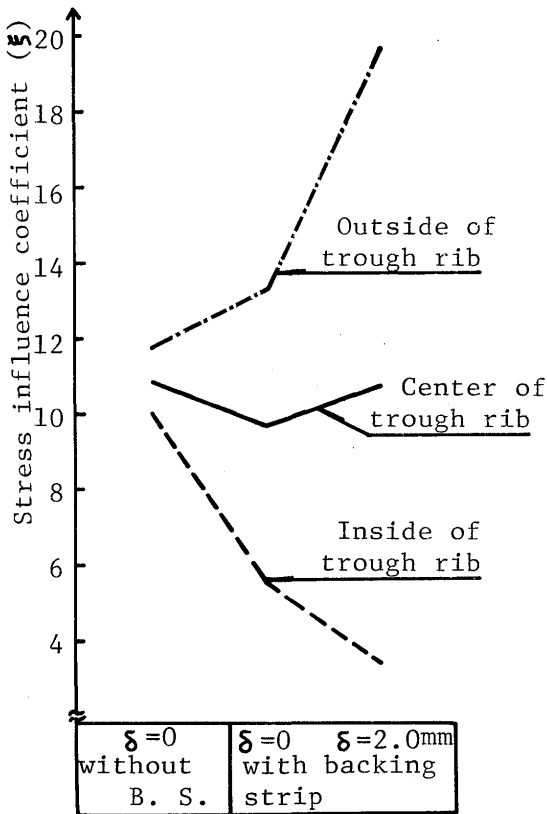


Fig. 16 Stress influence coefficient (ξ)

4.2 FEM Analysis of tensile specimen model

Fatigue crack both of full scale specimen and tensile specimen was initiated from weld root. Misalignment becomes the partial moment that is Stress Discontinuities as shown in Fig. 17a b).

Therefore, Finite-element analysis was used to the stress concentration ratio of root of trough rib flange, by changing misalignment (δ) and root angle (θ) of tickness direction of trough rib flange, as shown in Fig. 17c) d) e). Fig. 17e) indicates the black portion of c), and also allow size be equivalent to stress concentration ratio (α). Table 4 shows stress concentration ratio for nominal stress (=1 Kg/mm²) of mesh I, II, III. The relationship between α and δ was shown in Fig. 18, and α-θ was described in Fig. 19.

Result and discussion

- 1) In both upper free model and upper fixed model, the stress concentration ratio (α) is increased, as misalignment (δ) becomes larger.
- 2) When having same root angle (θ), misalignment (δ) greatly influences on stress concentration ratio (α).
- 3) The effect of misalignment (δ) is great. However, the influence of stress concentration ratio (α) for the

changing of root angle (θ) is not so great as the influence of misalignment (δ) (Fig. 19).

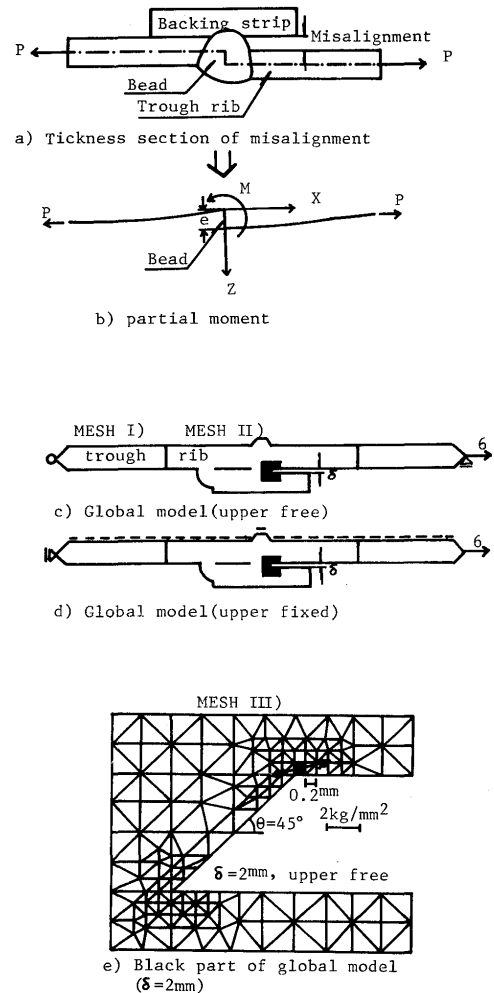


Fig. 17 Partial moment, FEM model

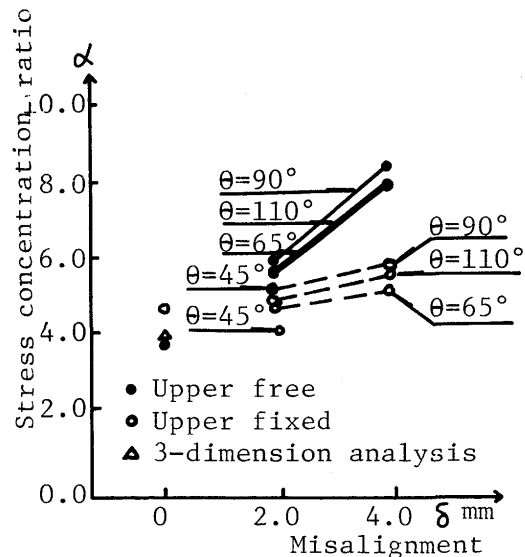


Fig. 18 α~δ curve

Table 4 Stress concentration, number of elements and nodal points for mesh I, II, III

Condition	Misalignment (mm)	Angle (°)	MESH										
			I			II			III			α	
			EL.	NO P.	S. EL.	EL.	NO P.	S. EL.	EL.	NO P.	S. EL.		
UPPER FREE	0	0	311	201	1.0	286	180	0.5	98	150	0.2	4.14	
		45	311	201	1.0	309	193	0.5	226	143	0.2	5.57	
		65	"	"	"	312	195	0.5	232	146	0.2	6.04	
		90	"	"	"	309	193	0.5	166	110	0.2	6.27	
	2	110	"	"	"	309	193	0.5	170	113	0.2	6.02	
		65	315	204	"	328	204	0.5	255	161	0.2	8.32	
		90	"	"	"	328	204	0.5	198	130	0.2	8.69	
		110	"	"	"	328	204	0.5	198	130	0.2	8.22	
	UPPER FIXED	0	0	311	201	"	286	180	0.5	98	150	0.2	5.03
			45	"	"	"	309	193	0.5	226	143	"	4.45
			65	"	"	"	312	195	0.5	232	146	"	5.09
			90	"	"	"	309	193	0.5	166	110	"	5.50
2		110	"	"	"	309	193	0.5	170	113	"	5.35	
		65	315	204	"	308	204	0.5	255	161	"	5.56	
		90	"	204	"	"	"	0.5	198	130	"	6.18	
		110	"	"	"	"	"	0.5	198	130	"	6.01	

EL.=Number of elements NO.P.=Number of nodal points S. EL.=Smallest Element size(mm)
 α =Stress concentration ratio

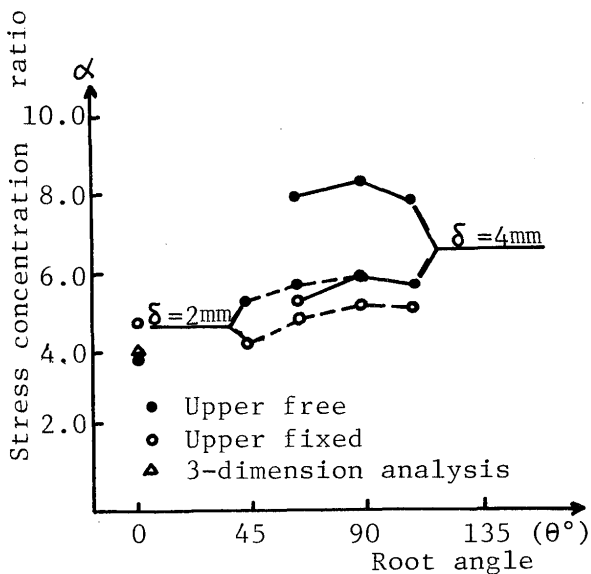


Fig. 19 $\alpha \sim \theta$ curve

5. Conclusion

Finally the aim of this research work is stated again:

Experimentally, the location of crack initiation was investigated by full scale bending fatigue specimen and tensile fatigue specimen. In the above model, the elastic analysis of stress concentration employed the Finite-element method.

1. Fatigue life was affected by the misalignment that is partial moment.
2. There were various shapes of weld root under the same welding condition.
3. As the misalignment becomes larger, the fatigue life was shorten.
4. According to macro section, several weld defects was

involved in fusion zone, but they were not always crack initiation.

5. The relationship between fatigue life and X-ray radiography classification was not distinct.
6. The cracks of all specimens were initiated from the weld root of trough rib flange.
7. According to FEM analysis of full scale model, shear deformation was involved in the corner of trough rib.

Acknowledgements

Specimens was manufactured from MITSUBISHI heavy industries, LTD.

The authors wish to acknowledge the helpful comments and suggestions of Dr. H. NAKAGAWA, Research Instructor for fractographic. Thanks are also due to Mr. H. SUZUKI, Research Associate for helpful FEM analysis and Mr. Y. Nakatsuji, Technical Assistant for helpful performing experiments, Welding Research Institute of Osaka University.

Finally, the authors is grateful to the HAN SHIN expressway public corporation for supporting of the investigation.

References

- 1) J.T. Oden: Mechanics of Elastic Structures, 1967, P.107-124.
- 2) A. Kondo, K. Yamada, Y. Kikuchi, K. Miyagawa and H. Aoki: IABSE Colloquium Lausanne, 1982, P.782-4.
- 3) K. Horikawa, D.U. Lee and H. Ishizaki: Proceedings of the 37th Annual Conference of the Japan Society of Civil Engineers, 1, Oct. 1982, P.145-146 (In Japan).
- 4) Japan Welding Soc.: Fractographic Atlas of Steel Weldments, 1982, P.378-380.

- 5) I. Soya, H. Kashimura, Y. Hagiwara, M. Sato and K. Minami: On the Brittle Fracture Initiation from a Surface Crack at Welded Joint. JSNA, Japan Vol. 140, 1976.
- 6) Albrecht, P.: "A Study of Fatigue Striations in Weld Toe Crack", Fatigue Testing Weldments, ASTM STP 648, D.W. Hoepfner, Ed., 1978, P.207-216.
- 7) K. Horikawa, D.U. Lee and H. Ishizaki: Proceedings of the 38th Annual Conference of the Japan Society of Civil Engineers, 1, Sep. 1983, P.303-304 (In Japan).
- 8) S.P. Timoshenko and J.N. Goodier: Theory of Elasticity, 3rd Edition, 1979, P.267-8.